

Synthesis and Structural Analysis of BaCrS₂

Omar Fuentes, Chong Zheng,* Catherine E. Check, Jianhua Zhang, and Gerardo Chacon

Department of Chemistry and Biochemistry, Northern Illinois University, DeKalb, Illinois 60115

Received June 1, 1998

A new ternary chromium sulfide, BaCrS₂, was synthesized. This solid state compound crystallizes in the orthorhombic, centrosymmetric space group *Pmnm* (No. 59) with $a = 4.2606(6)$ Å, $b = 4.7944(7)$ Å, $c = 9.443(1)$ Å, $V = 192.89(5)$ Å³, and $Z = 2$. The solid is similar to a previously known structure BaNiS₂ in which the Ni atom is coordinated to five sulfur atoms in a square pyramidal fashion. In BaCrS₂, the square pyramid distorts such that the two S(basal)–Cr–S(basal) angles are no longer equal. Thus the BaCrS₂ solid is orthorhombic whereas BaNiS₂ is tetragonal. The distortion from the square pyramidal coordination in the title compound is traced to the broken degeneracy of the d_{xy} and d_{xz} set by a computational analysis.

Introduction

Numerous ternary transition metal sulfides of the stoichiometry $A_xM_mS_n$ exist where A is an alkaline earth metal and M a group 5 or 6 transition metal. Examples include BaVS₃, Ba_{0.5}V₅S₈, Ba₉Nb₄S₂₁, and the well-known Chevrel phases SrMo₆S₈ and BaMo₆S₈.^{1–4} However, not many compounds of this type where M is the transition metal Cr have been synthesized. The single-crystal study on Ba_{0.51}Cr₅S₈ is the only one that has been reported in the literature.² Another compound, BaCr₂S₄, was also investigated,^{5,6} but its structure has not been fully characterized. In this contribution, we describe the synthesis, the structural determination, and a computational study of a ternary compound BaCrS₂.

Experimental Section

The synthesis was carried out in two steps. In the first step, elemental Ba (Atomergic Chemicals, 99.5%, cut pieces), Cr (Fisher, >99%, powder), and Sn (Fisher, >99%, powder, used as flux) were placed in a quartz ampule in the molar ratio of 1.5:3:6. The total weight of the sample was approximately 1.1 g. The quartz ampule was evacuated to about 10⁻⁴ Torr and sealed. A computer-controlled furnace was used to heat the ampule from room temperature to 1100 °C in 72 h, and this temperature was maintained for 96 h. The ampule was then cooled from 1100 °C to room temperature in a period of 96 h. In the second step, the product of the first reaction was ground and mixed together with 0.170 g of BaS (Alfa, 99.7%) and 3 g of KCl (Fisher, >99%, acted as flux). The KCl flux was previously dried at 250 °C under vacuum over a period of 48 h. The handling of the Ba metal and the KCl flux was inside an Ar-filled glovebox. The sample was placed in an evacuated (10⁻⁴ Torr) quartz ampule, sealed, and heated to 300 °C immediately. The temperature of the sample was raised from 300 to 900 °C in 24 h and maintained at 900 °C for 72 h. The sample was then cooled from 900 °C to room temperature over a period of 48 h. Gray, platelike crystals could be found in the final product after the

Table 1. Crystal Data and Structure Refinement for BaCrS₂

empirical formula	BaCrS ₂
fw	253.46
temp	293(2) K
wavelength	0.710 73 Å
cryst syst	orthorhombic
space group	<i>Pmnm</i> (No. 59)
unit cell dimens	$a = 4.2606(6)$ Å $b = 4.7944(7)$ Å $c = 9.4429(13)$ Å
vol, Z	192.89(5) Å ³ , 2
density (calcd)	4.364 Mg/m ³
abs coeff	13.784 mm ⁻¹
final R indices ^a [$I > 2\sigma(I)$]	R1 = 0.0335, wR2 = 0.0808
R indices (all data)	R1 = 0.0381, wR2 = 0.0831

$$^a R1 = \sum ||F_o| - |F_c|| / \sum |F_o|; wR2 = [\sum [w(F_o^2 - F_c^2)^2] / \sum [w(F_o^2)^2]]^{1/2}.$$

KCl flux was washed off and the sample dried in an oven. The whole procedure was repeated twice, and the same product was present in both samples.

Several crystals of the compound were indexed on a Siemens SMART CCD diffractometer using 40 frames with an exposure time of 20 s per frame. All of them exhibited the same orthorhombic cell. One crystal with good reflection quality was chosen for data collection. A total of 1224 reflections were collected in the hemisphere of the reciprocal lattice of the orthorhombic cell, of which 290 were unique with $R(\text{int}) = 0.0453$. An empirical absorption correction using the program SADABS⁷ was applied to all observed reflections. The structure was solved with direct methods using the SHELXS and SIR92 programs;^{7,8} both programs yielded the same structure. Full matrix least-squares refinement on F^2 was carried out using the SHELXL-93 program.⁷ The final agreement factor values are $R1 = 0.0335$, $wR2 = 0.0808$ ($I > 2\sigma$). The final structure was checked for additional symmetry with the MISSYM algorithm⁹ implemented in the PLATON program suite.¹⁰ No additional symmetry was found. The unit cell information and refinement details are reported in Table 1. The atomic positions and equivalent isotropic displacement parameters are listed in Table 2. Selected bond lengths and angles are in Table 3.

Semiquantitative EDAX analysis using the microprobe of a JEOL 35 CF-KeveX μx 7000 scanning electron microscope confirmed the

* To whom correspondence should be addressed. Telephone: (815) 753-6871. FAX: (815) 753-4802. E-mail: zheng@cz2.chem.niu.edu.

- (1) Gardner, R. A.; Vlasse, M.; Wold, A. *Acta Crystallogr. B* **1969**, *25*, 781.
- (2) Petricek, S.; Boller, H.; Klepp, K. O. *Solid State Ionics* **1995**, *81*, 183.
- (3) Saeki, M.; Onoda, M. *Bull. Chem. Soc. Jpn.* **1991**, *64*, 2923.
- (4) Kubel, F.; Yvon, K. *Acta Crystallogr. C* **1987**, *43*, 1655.
- (5) Brouwer, R.; Jellinek, F. J. *Chem. Soc., Chem. Commun.* **1977**, 879–880.
- (6) Omloo, W. P. F. A. M.; Jellinek, F. *Recl. Trav. Chim. Pays-Bas* **1968**, *87*, 545–548.

- (7) Sheldrick, G. M. *SHELXL*, version 5; Siemens Analytical Instruments Inc.: Madison, WI, 1994.
- (8) Altomare, A.; Cascarano, G.; Giacovazzo, C.; Guagliardi, A.; Burla, M. C.; Polidori, G.; Camalli, M. *J. Appl. Crystallogr.* **1994**, *27*, 435.
- (9) Le Page, Y. J. *J. Appl. Crystallogr.* **1987**, *20*, 264.
- (10) Spek, A. L. *Acta Crystallogr., Sect. A: Found. Crystallogr.* **1990**, *46*, C34.

Table 2. Atomic Coordinates ($\times 10^4$) and Equivalent Isotropic Displacement Parameters ($\text{\AA}^2 \times 10^3$) for BaCrS_2 ^a

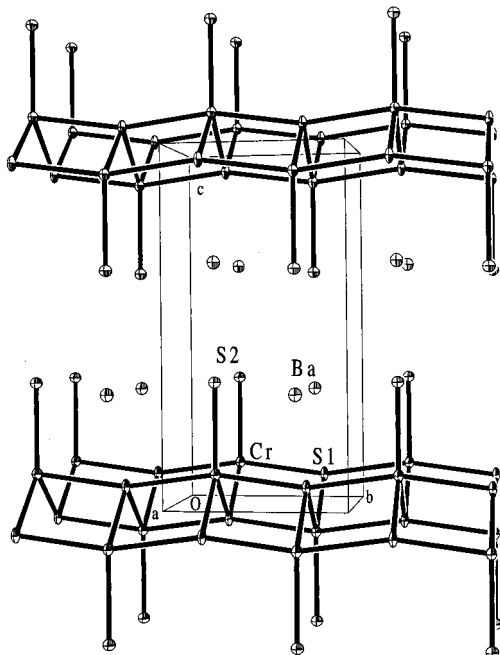
	<i>x</i>	<i>y</i>	<i>z</i>	<i>U</i> (eq)
Ba	2500	-2500	3225(1)	13(1)
Cr	7500	2500	906(2)	14(1)
S(1)	7500	-2500	557(4)	13(1)
S(2)	7500	2500	3473(3)	13(1)

^a *U*(eq) is defined as one-third of the trace of the orthogonalized U_{ij} tensor.

Table 3. Selected Bond Lengths (\AA) and Angles (deg) for BaCrS_2 ^a

Ba-S(2)#1	3.119(3)
Ba-S(2)	3.2155(4)
Ba-S(1)	3.299(3)
Cr-S(1)	2.4198(7)
Cr-S(2)	2.424(4)
Cr-S(1)#5	2.539(2)
Cr-Ba#6	3.8829(13)
Cr-Ba#5	3.900(2)
S(1)-Cr-S(1)#6	164.3(2)
S(1)#6-Cr-S(2)	97.84(10)
S(1)-Cr-S(1)#5	85.74(5)
S(2)-Cr-S(1)#5	122.96(8)
S(1)#5-Cr-S(1)#7	114.1(2)

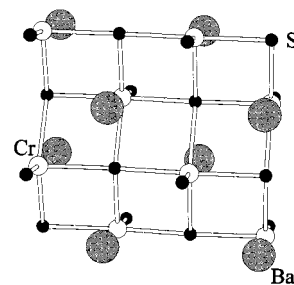
^a Symmetry transformations used to generate equivalent atoms: #1, $-x + 1, -y, -z + 1$; #5, $-x + 1, -y, -z$; #6, $x, y + 1, z$; #7, $-x + 2, -y, -z$.

**Figure 1.** BaCrS_2 structure viewed down the *a*-axis. Thermal ellipsoids of 50% probability are plotted.

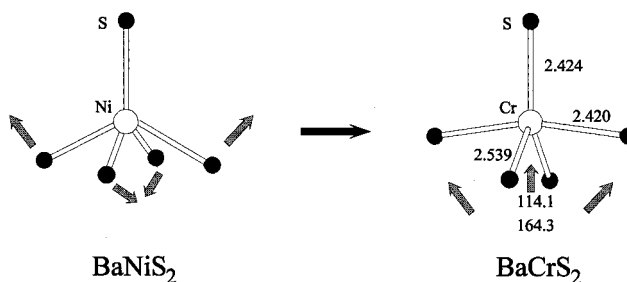
presence of all three elements in the same crystal used for X-ray data collection. Sn, K, and Cl were not observed within the detection limits of the instrument.

Results and Discussion

Structure. Figure 1 shows the BaCrS_2 structure. It consists of CrS_2 layers separated by Ba sheets. Within the layer, the Cr atom is coordinated to five S atoms. We can refer to four (S1) of the five S atoms as "basal" and one (S2) as "apical", although the coordination motif is a significantly distorted square pyramid. The bonding of the Cr atom to the S1 atoms can be visualized as a sheet of a distorted and puckered square lattice

**Figure 2.** Top view of the BaCrS_2 layer. The large shaded circles are Ba, the medium open circles Cr, and the small solid circles S.

Scheme 1

**Table 4.** Extended Hückel Parameters^a

	orbital	H_{ii} (eV)	ζ_1^b	ζ_2	c_1^b	c_2
Ba	6s	-7.0	1.2			
	6p	-4.0	1.2			
Cr	4s	-8.66	1.7			
	4p	-5.24	1.7			
	3d	-11.22	4.95	1.8	0.5060	0.6750
S	3s	-20.0	1.817			
	3p	-13.3	1.817			

^a References 20–22. ^b Exponents and coefficients in a double ζ expansion of the d orbital.

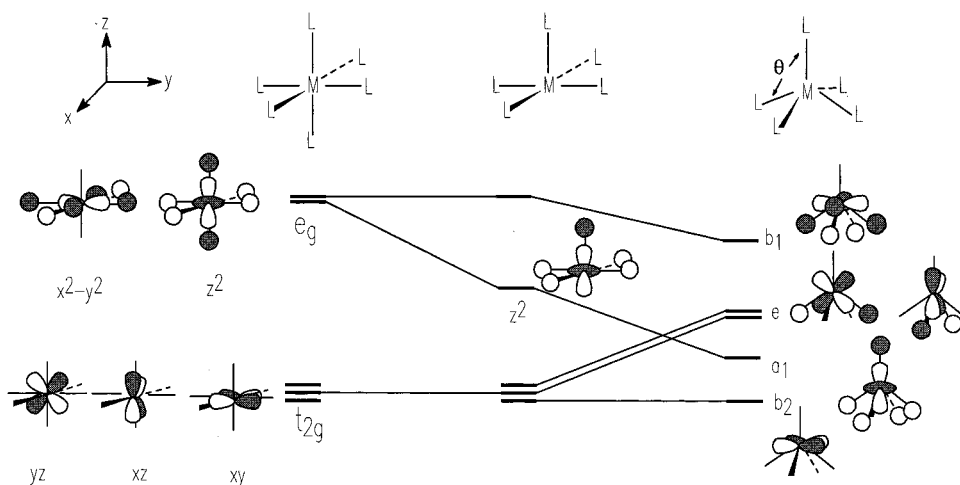
of S atoms with Cr atoms capping from above and below the hollows. Figure 2 demonstrates such a view. The lengths of the two types of bonds from the capping Cr to the S1 atoms are 2.420 and 2.539 \AA , respectively. They are slightly larger than the sum of the covalent radii of Cr (1.24 \AA) and S (1.03 \AA). The apical S2 atom bonds to the Cr atom with a distance of 2.424 \AA . The layers are stacked in the direction of the *c*-axis of the lattice.

The structure can be considered as a distorted BaNiS_2 type.¹¹ In the tetragonal BaNiS_2 , Ni is at the center of a square pyramid of a S_5 unit. The basal S atoms form a planar square net with the Ni atom capping from above and below the square hollows. The basal Ni-S bond length is 2.34 \AA and the apical 2.31 \AA . The S(basal)-Ni-S(basal) angle is 141.6°. The distortion from the BaNiS_2 type to the BaCrS_2 type at the metal center is schematically depicted in Scheme 1, where one of the S(basal)-Ni-S(basal) angles closes from 141.6 to 114.1° and the other opens to 164.3°. For clarity, the larger angle is shown parallel to the paper.

The actual local environment of the metal center in the BaCrS_2 structure is shown on the right side of Scheme 1 (bond lengths in angstroms and angles in degrees). At this metal center, there are three types of Cr-S bonds: two Cr-S1 and one Cr-S2.

Computational Analysis. To understand the difference between the BaCrS_2 and the BaNiS_2 structures, we computed the band structure and the crystal orbital overlap population

Scheme 2



(COOP) curves using the tight-binding extended Hückel method.^{12–14} The parameters used in the computation are listed in Table 4. A set of 125 k-points in the irreducible wedge of the Brillouin zone was employed in the computation of the COOP curves. The electronic structure of a transition metal at the center of a S₅ pyramid is well-known¹⁵ and can be derived from that of an octahedrally coordinated complex by first removing an apical ligand and then changing the L(basal)–M–L(basal) angle from 90° to about 110° for an idealized tetragonal BaCrS₂ structure. This process and the accompanying orbital evolution are shown in Scheme 2. When an apical ligand is removed, the d_{z²} orbital comes down in energy because there is less antibonding interaction with the ligands. When the L(basal)–M–L(basal) angle is changed, the d_{xy} orbital is not affected since it avoids the directions of the ligands, but the d_{xz} and d_{yz} orbitals go up in energy because the basal ligands are now pointing to the lobe directions of these orbitals and therefore enhance the antibonding interaction. The d_{z²} and d_{x²–y²} come down in energy because the ligands are now not pointing to the directions of orbital lobes and the antibonding character is thus reduced.

The effect on the orbitals of the distortion shown in Scheme 1 is schematically illustrated in Scheme 3 (the larger angle is now perpendicular to the paper to be consistent with the crystallographic coordinate system). When the L(basal)–M–L(basal) angle opens up to 164.3° (the actual angle in the BaCrS₂ structure) in the xz plane, the d_{xz} orbital goes down in energy. This is because the ligands now move closer to the xy nodal plane of the d_{xz} orbital, and there is less overlap between the d_{xz} and the ligand orbitals and thus less antibonding character. When the L(basal)–M–L(basal) angle closes to 114.1° (also the actual angle in the BaCrS₂ structure) in the yz plane, the d_{yz} orbital goes up in energy because the orbital overlaps better with the ligands (the maximum overlap occurs at 90°). Because of the distortion, the HOMO is of weak metal–ligand antibonding character for a d⁴ configuration (corresponding to a formal electron partitioning of Ba²⁺Cr²⁺(S²⁻)₂). Figure 3 shows the computed COOP curves of the two types of Cr–S bonds. Indeed, the states near the Fermi level are of weak metal–ligand antibonding nature.

Scheme 3

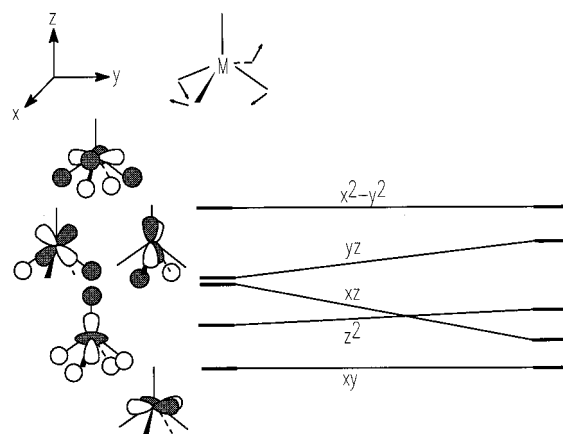


Figure 4 shows the computed band structure of an idealized tetragonal BaCrS₂ lattice (using the *b*-axis of the actual BaCrS₂ structure as the *a*- and *b*-axes). In the direction of the Z (0, 0, 0.5) to the Γ (0, 0, 0) point in the Brillouin zone, the bands are flat while those in the direction of Γ to M (0.5, 0.5, 0) have appreciable dispersion. This is because the interaction is weaker between the layers than within the layer of the BaCrS₂ structure. There are two metal atoms in the unit cell, thus 10 d bands in the plot. The pair of each metal d orbital type forms in-phase (+) and out-of-phase (–) combinations. The lowest d band is the in-phase combination of the metal d_{xy} orbitals, xy (+), because the d_{xy} orbital is mainly nonbonding (see Scheme 3). Next comes the out-of-phase (–) combination of the d_{xy} orbital, xy (–). The degenerate sets xz, yz (+) and xz, yz (–) are very close in energy since the overlap between them is poor and therefore the linear combination does not separate them much. However, the x² – y² (+) and x² – y² (–) bands show much larger energy separation. This is because of their interaction with the ligand orbitals (see Scheme 4). At the Γ point, there are two bonding and two antibonding contacts at each ligand center for the x² – y² (+) orbital, but four antibonding contacts for the x² – y² (–) orbital. Thus the energies of these two bands are very different. A similar situation occurs for the z² (+) and z² (–) bands. From Scheme 4, the degeneracy of the x² – y² (+) and the x² – y² (–) orbitals at the M point can also be understood. Both have the same nodal character, and a 90° rotation transforms one orbital to the other.

Figure 5 is the computed band structure of the actual, orthorhombic BaCrS₂ lattice. Because of the orbital evolution

(12) Hoffmann, R. *J. Chem. Phys.* **1963**, *39*, 1397.

(13) Whangbo, M.-H.; Hoffmann, R.; Woodward, R. B. *Proc. R. Soc., London* **1979**, *A366*, 23.

(14) Wijeyesekera, S. D.; Hoffmann, R. *Organometallics* **1984**, *3*, 949.

(15) Albright, T. A.; Burdett, J. K.; Whangbo, M.-H. *Orbital Interactions in Chemistry*; Wiley: New York, 1985.

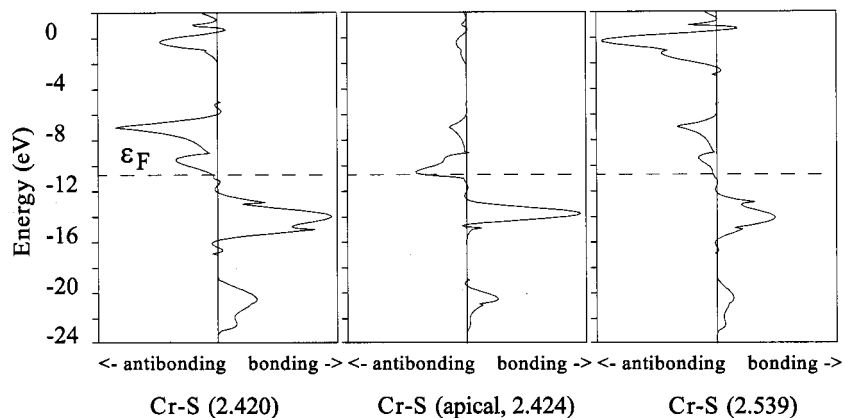


Figure 3. The computed COOP curves of the Cr-S bonds in the BaCrS₂ structure. The left is for one of the two types of Cr to basal S bonds (2.4203 Å), the middle one is for the Cr to apical S bond (2.4235 Å), and the right one is for the other type of the Cr to basal S bond (2.539 Å). The dashed horizontal line indicates the Fermi level.

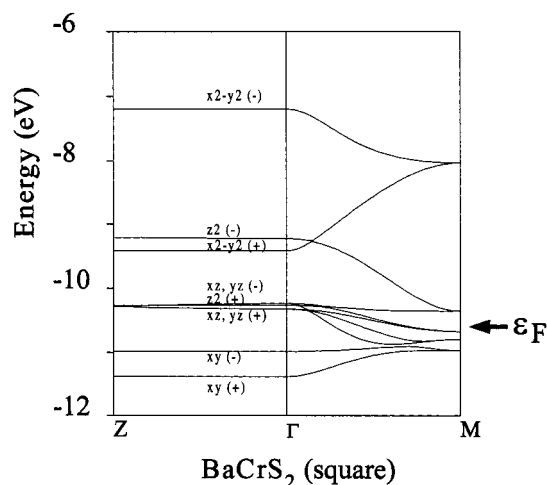
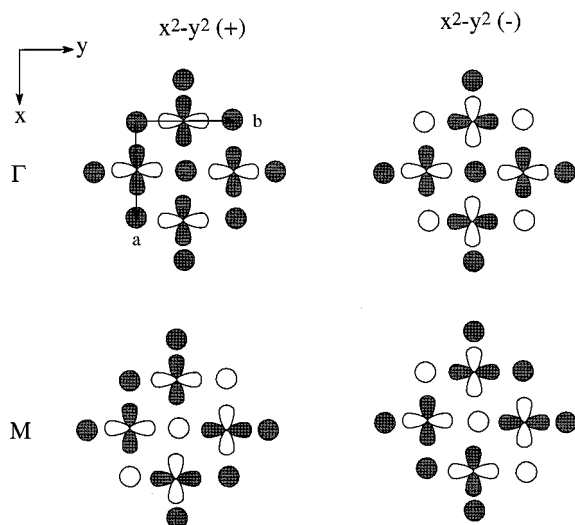


Figure 4. Computed band structure of an idealized tetragonal ($a = 4.794$ Å, $c = 9.443$ Å) BaCrS₂ compound. Only the d band region is shown. The three special k-points in the reciprocal lattice are Z [0, 0, 0.5], Γ [0, 0, 0], and M [0, 0.5, 0.5].

Scheme 4



accompanying the distortion from the idealized tetragonal lattice shown in Scheme 3, the degeneracy of the xz and yz bands is broken. A band gap of about 0.2 eV is opened up for a d^4 electronic configuration. The four bands below the Fermi level are occupied, and those above it are empty. Thus at the extended

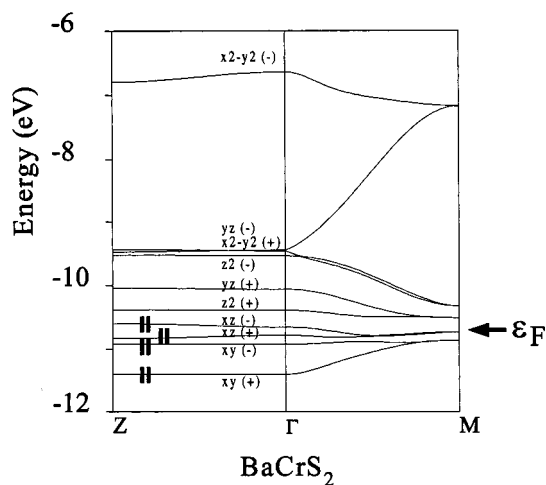


Figure 5. Computed band structure of the BaCrS₂ compound. Only the d band region is shown. The three special k-points in the reciprocal lattice are Z [0, 0, 0.5], Γ [0, 0, 0], and M [0, 0.5, 0.5]. The lowest four bands are occupied as indicated by the vertical bars.

Hückel level of computation, the compound is predicted to be a semiconductor. Notice that the degeneracy of the $x^2 - y^2$ (+) and the $x^2 - y^2$ (-) orbitals is maintained at the M point. This is because the two metal atoms in the unit cell (at the Wyckoff position 2b) are related to each other by two screw axes along the a and b directions. The orbital interaction pattern is similar to that of the tetragonal lattice shown in Scheme 4. The other pairs of bands are also degenerate at the M point, but there are avoided crossings and mixing between orbitals of different types due to the loss of the diagonal symmetry. Because of this degeneracy, there is no opening of a band gap for a d^8 (corresponding to $\text{Ba}^{2+}\text{Ni}^{2+}(\text{S}^{2-})_2$) or d^7 configuration. Therefore little stabilization is gained for a distortion from a tetragonal to an orthorhombic lattice. The extended Hückel method prefers the orthorhombic structure for both electronic configurations, but the energy difference is larger for the d^4 (0.83 eV) than for the d^8 configuration (0.27 eV).

It is interesting to note that two additional compounds of the group 9 transitional metal Co of the stoichiometry AMX_2

- (16) Jansen, M.; Hoppe, R. *Z. Anorg. Allg. Chem.* **1975**, *417*, 31–34.
- (17) Baenziger, N. C.; Grout, L.; Martinson, L. S.; Schweitzer, J. W. *Acta Crystallogr. C* **1994**, *50*, 1375–1377.
- (18) Snyder, G. J.; Gelabert, M. C.; DiSalvo, F. J. *J. Solid State Chem.* **1994**, *113*, 355–361.
- (19) Gelabert, M. C.; Brese, N. E.; DiSalvo, F. J.; Jobic, S.; Deniard, P.; Brec, R. *J. Solid State Chem.* **1996**, *127*, 211–221.

possessing the pyramidal structural motif adopt a tetragonal lattice. These are BaCoS₂ and KCoO₂.¹⁶ BaCoS₂ is polymorphic and crystallizes in three different types of lattices: monoclinic,¹⁷ orthorhombic,¹⁸ and tetragonal.¹⁹ Only the orthorhombic and tetragonal lattices have the pyramidal structural motif that is in BaCrS₂. The metal local coordination in the orthorhombic lattice has merely a small distortion from a square pyramidal geometry. All four metal to basal S distances are equal (2.434 Å); only the two types of acute S(basal)-Co-S(basal) angles are slightly different. One is 82.9° and the other 83.7°. There, as far as the local metal coordination is concerned, the orthorhombic phase is equivalent to that of the tetragonal.

(20) Zheng, C. *J. Am. Chem. Soc.* **1993**, *115*, 1047.

(21) Summerville, R. H.; Hoffmann, R. **1976**, *98*, 7240.

(22) Chen, M. M. L.; Hoffmann, R. *J. Am. Chem. Soc.* **1976**, *98*, 1647.

Conclusions

The group 6 transition metal ternary sulfide compound BaCrS₂ has been synthesized and analyzed. The computed band structure suggested that it should be a semiconductor. Further study on the transport properties of the title compound will be carried out in the future once large enough crystals can be grown.

Acknowledgment. We thank Robert L. Bailey of the Department of Geology at Northern Illinois University for the assistance of the microprobe measurement. We also thank the National Science Foundation for the support of our research through Grant DMR-9704048.

Supporting Information Available: One X-ray crystallographic file, in CIF format, is available. This material is available free of charge via the Internet at <http://pubs.acs.org>.

IC980609P